OXFORD

Journal of Geophysics and Engineering

Journal of Geophysics and Engineering (2019) **16**, 559–570 doi:10.1093/jge/gxz027

Mechanisms behind strong strata behaviour in high longwall mining face-ends under shallow covers

Weibing Zhu[1], **Xiangrui Qi**[1], **Jinfeng Ju**[2,*] **and Jingmin Xu**[3]

[1] Key Laboratory of Deep Coal Resource Mining, Ministry of Education of China; School of Mines, China University of Mining and Technology, Xuzhou, 221116, China
[2] IoT/Perception Mine Research Center, China University of Mining and Technology, Xuzhou, Jiangsu 221008, China
[3] Department of Civil Engineering, Faculty of Engineering, University of Nottingham, University Park, Nottingham NG7 2RD, United Kingdom

*Corresponding author: Jinfeng Ju. E-mail: jujinfeng2012@163.com

Received 29 August 2018, revised 10 March 2019
Accepted for publication 1 April 2019

Abstract

Safe and efficient mining of shallow coal seams relies on the understanding and effective control of strata behaviour. Field measurements, theoretical analysis and numerical simulations are presented in this study to investigate the mechanism behind abnormal strata behaviour, such as roof collapse and severe roadway deformation, that occurs in high longwall face-ends under shallow cover. We observed that coal pillars with two sides being mined out become unstable when the cover depth exceeds a certain value. The instability of the coal pillar can alter the fracture line of the overlying strata, triggering a reversed rotation of the 'curved triangle blocks' that form after the breakage of the overlying main roof. The revolving blocks apply stress on the roof strata directly above the longwall face-end, resulting in roof collapse. The collapse of both the coal pillars and the roof also leads to the advancement and increase of the overlying abutment pressure, which further causes severe roadway deformation in front of the working face. The strong strata behaviour that occurs in high longwall face-ends with shallow cover is presented in this study and countermeasures are proposed, such as widening or strengthening the coal pillar, or implementing destress blasting. The countermeasures we proposed and the results of our analyses may facilitate the safe mining of shallow coal seams with similar problems in the future, and may improve the safety and efficient working of coal mines.

Keywords: shallow coal seam, coal pillar, strong strata behaviour, longwall face-end, curved triangle block

1. Introduction

Underground coal mining inevitably causes strata movement and ground subsidence unless backfill mining is implemented (Xuan *et al.*, 2015, 2017; Zhu *et al.* 2017c). The stress transfer/relief during mining is the root cause of mine pressure (Peng 1978; Xie *et al.* 2018; Zhu *et al.* 2018b), and a critical factor in safe and efficient mining is to control and make use of mine pressure in a scientific and rational manner. It is generally believed that the high stresses caused by deep mining are the dominant factor leading to the occurrence of strong mine pressure on roadways (Malan 1998; He *et al.* 2005), whereas severe strata breakage and movement during extraction lead to strong mine pressure in working faces (Bieniawski 1986; Qian *et al.* 2010). In major coal mining countries such as China and Australia, coal output mainly comes from the exploitation of shallow coal resources (Huang 2002; Mudd 2010; Meng *et al.* 2016; Xu *et al.*

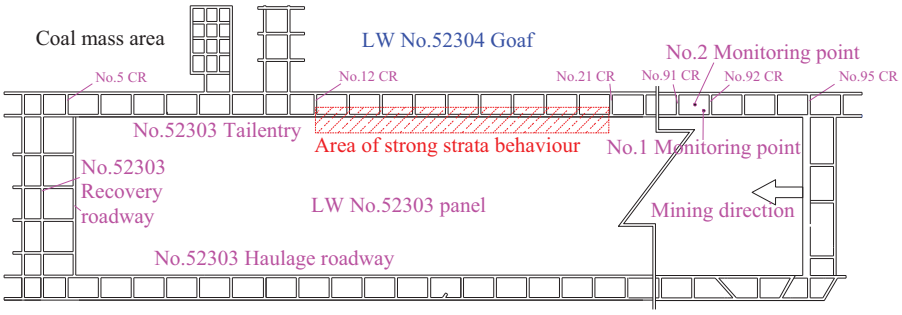

Figure 1. Roadway layout of longwall No. 52 303 and the area of strong strata behaviour.

2017). Hence, investigating the mechanisms driving strata behaviour in shallow coal seam mining is of the utmost importance.

In this study, discussion of shallow coal seams is generally in reference to coal seams with a cover depth of less than 300 m, such as the coal seams in the Shendong coalfield, located in the northwest part of China (Ju *et al.* 2015b). Shallow coal seam mining is generally practised at high intensity, with high mining heights and fast advancing speeds. Case studies of engineering practices have demonstrated that strata behaviour in shallow coal seam mining is relatively severe, regardless of how shallow the coal seams are (Xu *et al.* 2014, 2017; Zhu *et al.* 2015, 2017b, 2018a,c; Ju *et al.* 2015a,b). Numerous mining case studies in the Shendong coalfield have demonstrated that under specific mining conditions, strong strata behaviour, such as sudden roof subsidence, or even support failure incidents, are triggered very easily when longwall faces advance beneath valley terrain (Xu *et al.* 2012), thin bedrock with thick windblown sand (Hou 2000; Zhu 2011) or deserted upper coal pillars (Ju *et al.* 2015b; Xu *et al.* 2017). Previous researchers (Hou 2000; Zhu 2011; Xu *et al.* 2012, 2017; Ju *et al.* 2015b) studied the mechanisms and prevention of these particular types of strong strata behaviours and have achieved remarkable results. Due to the small stress formation in shallow coal seams, strata behaviour in roadways is relatively moderate. Therefore, strong strata behaviour in roadways in shallow coal seam mining has rarely been reported (Zhu *et al.* 2017a).

In longwall mining, the specific breakage forms and movement characteristics of the overlying strata cause the intensity of strata behaviour in the centre of the working face to be more severe than that of the behaviour at the working face-end (Qian *et al.* 2010). In one longwall face of the Daliuta coal mine in the Shendong mining area, strong strata behaviours such as roof collapse and sudden roof subsidence have occurred at the working face-end, though these phenomena were clearly exceptional. Additionally, phenomena, such as advance floor heave, rib spalling and roof subsidence have occurred in the roadways, triggering several breakages and inclination incidents in the individual advance props. The abnormally strong mine pressures have not only brought confusion to underground workers, but have also seriously affected the safe and efficient production of the working face. Although some papers (Yang and Liu 2012, Yang *et al.* 2016) have studied strong strata behaviour occurring in a fully mechanized top-coal caving working face-end, the mechanisms behind abnormally strong strata behaviour in a fully mechanized longwall face-end have been difficult to explain.

This study presents theoretical analysis, numerical simulation and field measurements to investigate the mechanisms behind strong strata behaviour in high longwall face-ends with shallow covers, and corresponding countermeasures are proposed. The results are expected to facilitate the safe mining of shallow coal seams with similar problems in the future.

2. Strong strata behaviour in working face-ends

2.1. *Case study of working face mining conditions*

Longwall No. 52 303, a fully mechanized working face with a high mining height, was the second mining face of the No. 3 district in the No. 5-2 coal seam of the Daliuta coal mine, in the Shendong mining area. The width of the coal pillars between longwalls No. 52 303 and No. 52 304 was 20 m, as shown in figure 1. The width and length of longwall panel No. 52 303 were 301.5 and 4443.3 m, respectively, with a designed mining height of 6.6 m. The thickness of the coal seam ranged from 6.6 to 7.3 m, with an average value of 6.9 m. The coal seam was sub-horizontal, with a dip angle ranging from 1° to 3°. The cover depth of the coal seam ranged from 173 to 282 m, with the thickness of the overlying bedrock ranging from 132 to 245 m. The immediate roof of the coal seam was stable and intact, and included a sequence of fine sandstone and mudstone. The strata column section of the longwall No. 42 303 is shown in Table 1, where T is the thickness of strata and D is the depth of strata.

Most of the surface of longwall No. 52 303 is covered by quaternary loose sediments and bedrock outcrops can be seen in gully areas, but the gully development area in the

Table 1. Strata column section of the longwall No. 52 303.

No.	*T (m)*	*D (m)*	Lithology	Columnar	No.	*T (m)*	*D (m)*	Lithology	Columnar
1	4.78	4.78	Drift-sand						
2	1.90	6.68	Packsand		29	8.98	83.58	Siltstone	
3	0.35	7.03	Seam 2-2		30	3.00	86.58	Sandstone	
4	1.32	8.35	Mudstone		31	9.24	95.82	Siltstone	
5	3.34	11.69	Packsand		32	1.15	96.97	Sandshale	
6	6.47	18.16	Siltstone		33	5.58	102.55	Siltstone	
7	0.66	18.82	Seam 2-2		34	1.30	103.85	Quartzite	
8	4.41	23.23	Siltstone		35	2.63	106.48	Siltstone	
9	1.00	24.23	Mudstone		36	0.44	106.92	Seam4-2	
10	3.65	27.88	Siltstone		37	6.09	113.01	Siltstone	
11	0.60	28.48	Sandstone		38	1.92	114.93	Sandstone	
12	3.85	32.33	Siltstone		39	4.92	119.85	Packsand	
13	0.89	32.33	Packsand		40	4.17	124.02	Siltstone	
14	3.00	36.22	Siltstone		41	1.50	125.52	Sandstone	
15	0.80	37.02	Mudstone		42	1.80	127.32	Siltstone	
16	1.55	38.57	Siltstone		43	0.60	127.92	Siltstone	
17	1.10	39.67	Mudstone		44	3.84	131.76	Packsand	
18	0.80	40.47	Packsand		45	1.55	133.31	Mudstone	
19	1.72	42.19	Siltstone		46	1.25	134.56	Sandstone	
20	1.70	43.89	Packsand		47	0.49	135.05	Packsand	
21	3.82	47.71	Siltstone		48	3.75	138.80	Siltstone	
22	0.35	48.06	Seam3-1		49	0.15	138.95	Seam 4-4	
23	3.55	51.61	Mudstone		50	3.50	142.45	Siltstone	
24	13.43	65.04	Sandstone		51	4.22	146.67	Packsand	
25	2.10	67.14	Sandshale		52	0.80	147.47	Calcarinate	
26	1.18	68.32	Packsand		53	27.64	175.11	Sandstone	
27	5.40	73.72	Siltstone		54	2.07	177.18	Siltstone	
28	0.88	74.60	Sandshale		55	7.14	184.32	Seam 5-2	

middle working face is thinner. In this district, some areas above coal seam No. 2-2 are prone to caving, and the lithology of the roof in these areas is argillaceous cementation, which easily develops a sliding face. No faults, scour bodies or other structures were found in the tunnelling process of the gate roadway of the working face.

2.2. *Characteristics of the strong strata behaviour*

During the operation of longwall No. 52 303, the impact of strata behaviour at the working face-end and advance support area of the tail-entry varied with the longwall face positions, as shown in figure 1, in which the connection roadway is abbreviated to CR.

Before longwall No. 52 303 advanced from the setup room to the No. 21 connection roadway (at a corresponding advancement distance of 3492 m), high roof pressure in an area with 20 total supports (approximately 40 m to the tail-entry of the working face) never occurred, nor did phenomena such as roof collapse or rib spalling. The overall conditions of the advance support areas at the tail-entry and head-entry were basically the same, with minor roadway deformation. However, when the working face was operated between the No. 21 and No. 12 CRs (corresponding to between 3492 and 3676 m in advancement distance), the working resistance of the 20 supports adjacent to the tail-entry significantly increased, as shown in figure 2, and incidents including roof collapse and coal-wall rib spalling became very severe at the working face-end.

At the same time, serious floor heave, rib spalling and roof subsidence occurred at the tail-entry within the region from 40 to 50 m in front of the working face. The quantities of floor heave, rib spalling and roof subsidence were 200–800, 800–1200 and 400–500 mm, respectively, and triggered several breakages and inclination incidents in the individual advance props, as shown in figure 3. However, during the advancement of the working face from No. 12 CR to the recovery roadway (No. 1 CR), the above-mentioned phenomena and incidents ceased, and the strata behaviours at the working face-end returned to normal again.

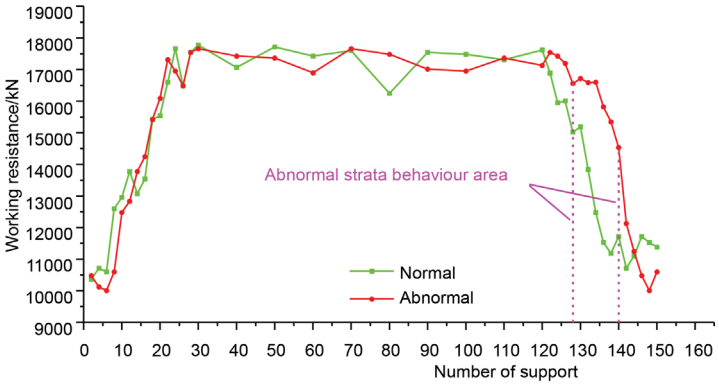

Figure 2. Comparison between the support resistances of normal and abnormal strata behaviours.

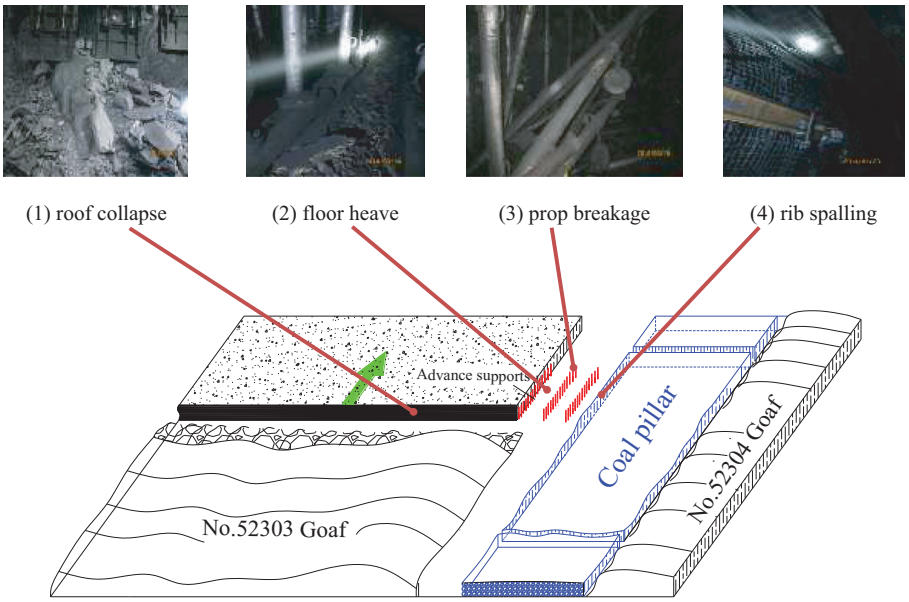

Figure 3. Sketch map of strong strata behaviour in the face-end.

Thus, the strata behaviour in the longwall No. 52 303 face-end is an exception to the general understanding of moderate strata behaviour at working face-ends, where the overlying strata weight is mainly supported by curved triangle blocks (defined in Section 3.1) that form after the hard roof breaks. It is worth noting that the abnormal strata behaviour at the face-end only occurred when longwall No. 52 303 advanced between the No. 21 and No. 12 CRs. Therefore, to prevent similar incidents in the future, understanding the mechanism driving this exceptional strong strata behaviour is critical.

3. Mechanism driving the strong strata behaviour

3.1. *Movement characteristic of the curved triangle block*

The strata behaviour of the working face is closely related to factors, such as the working resistance of the supports, surrounding geological conditions and mining parameters (Singh *et al.* 2008; Qian *et al.* 2010; Masoud *et al.* 2016; Li *et al.* 2018; Zhu *et al.* 2018a). The breakage and movement characteristics of the hard roof directly determine the strata behaviour in the working face. In other words, the weight of the overlying strata can be borne, and the movement of the overlying strata can be controlled by some thick and strong strata. These strata are termed key strata according to the key stratum hypothesis (Qian *et al.* 2010; Qu *et al.* 2015). In longwall mining, when the working face advances, the cracks of the overlying strata, which can be seen as thin plates, develop from both of the two long sides with the development of a central crack in the reverse of the plate. Three-pronged cracks then develop from the endpoints of the central crack, and extend further. Finally, 'O' shaped cracks are formed near the edges of the suspended plate and the 'X' shaped fracture line, which forms in the middle of the plate and further connects. As the working face advances, the key strata periodically break and continually form successive broken plates

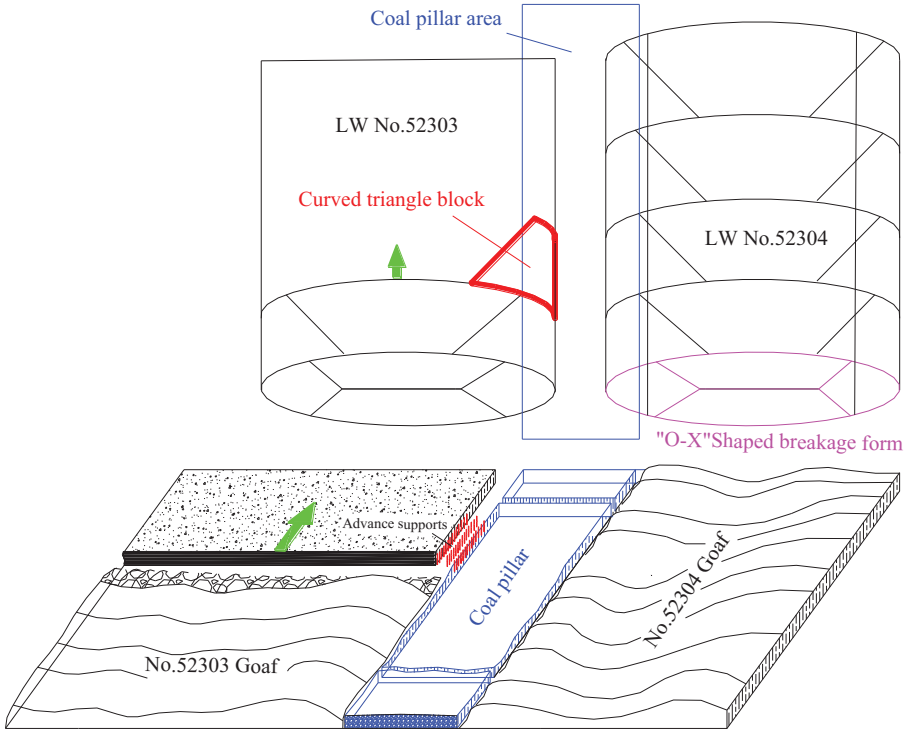

Figure 4. 'O-*X*' breakage of the overlying hard roof.

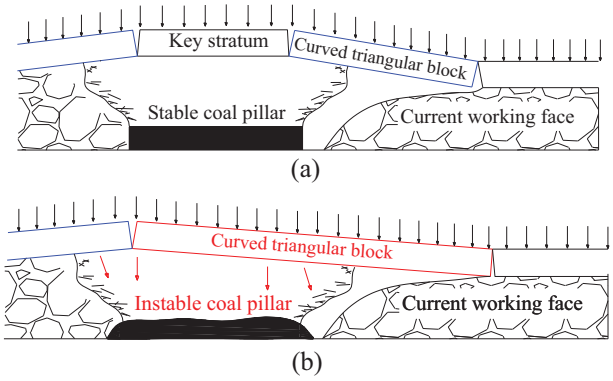

Figure 5. Movement characteristic of the curved triangle block in two situations: (a) coal pillar remains stable and (b) coal pillar loses stability.

(Qian *et al.* 2010; Xu *et al.* 2016; Yu *et al.* 2016; Han *et al.* 2018), as shown in figure 4.

Due to the restriction (bending moments) of the coal pillar to the overlying strata, when the coal mass or the pillars at the two ends of the working face are stable, the breakage line of the hard roof is on the side of the coal pillar connecting to the working face., where the resulting broken block above the working face-end, as shown in figure 5a, is termed the 'curved triangle block'. The two ends of the curved triangle block are mainly supported by the coal pillar (left end) and gangue (right end), respectively, as shown in figure 5a. Hence, under the protection of the curved triangle block, the strata behaviour at the working face-end is relatively moderate. However, when the coal pillar becomes unstable, the breakage shape of the hard roof and the movement characteristics of the curved triangle block will also be altered. As the unstable coal pillar cannot sufficiently restrict the rotation of the end of the hard roof (i.e. bending moment), the breakage line of the hard roof will move to the opposite side of the coal pillar, as shown in figure 5b. Moreover, the instability of the coal pillar gives rise to a reversed rotation of the triangle block, thereby crushing the immediate roof over the face-end and further triggering roof collapse. This further causes the advancement and increase of the overlying abutment pressure, thereby severely destroying the roadway in the advance support area. Thus, the stability of the coal pillar determines the breakage shape and the movement of the hard roof above the longwall face-end directly, affecting the strata behaviour accordingly.

Having observed the roadway deformation of longwall No. 52 303, it is reasonable to infer that the destruction of the coal pillar may cause strong strata behaviour at the working face-end. It is therefore necessary to investigate the stability of the coal pillars of the longwall No. 52 303 working face to understand the abnormal strata behaviour that occurred.

3.2. *Stability analysis of the coal pillar*

3.2.1. Width of the plastic zone of the coal pillar. According to the limit equilibrium theory, the width of the plastic zone of the coal pillar mined on one side, x_0, can be expressed as

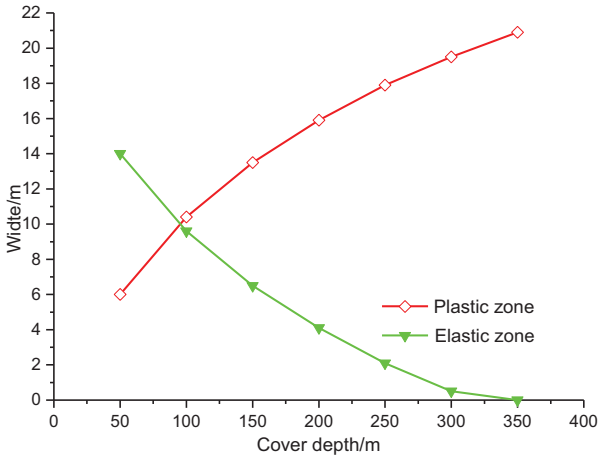

Figure 6. Plot of the plastic zone width of the coal pillar vs. cover depth.

(Bai 2006; Qian *et al.* 2010; Jia *et al.* 2011; Gao 2014):

$$x_0 = \frac{MA}{2\tan\phi_0}\ln\left(\frac{k\gamma H + \frac{C_0}{\tan\phi_0}}{\frac{C_0}{\tan\phi_0} + \frac{P_z}{A}}\right) \quad (1)$$

where M is the mining height of the working face; A is the coefficient of horizontal pressure; ϕ_0 is the angle of internal friction; k is the stress-concentration factor; γ is the average unit weight of the overlying strata; H is the cover depth of the working face; C_0 is the cohesion coefficient of the coal mass and P_z is the support resistance of the roadway.

When the coal pillar is subject to a second round of mining from another panel, as in the cases of most coal pillars between longwall No. 52 303 and longwall No. 52 304 for example, a disturbance factor of 1.2 is adopted for this analysis. Thus, the width of the plastic zone of the coal pillar mined on both sides, x, can be expressed as

$$x = x_0 + 1.2x_0 = 2.2x_0 \quad (2)$$

According to the field data obtained from the Daliuta coal mine and laboratory test results on coal samples from there, the relationship between the width of the plastic zone and the cover depth can be calculated using equations (1) and (2), the result of which is plotted in figure 6. In this calculation, the values of the parameters were as follows: $M = 7$ m, $A = 0.8$, $C_0 = 1.4$ MPa, $\varphi_0 = 30°$, $K = 2.0$, $\gamma = 0.025$ MN m^{-3} and $P_z = 0.3$ MPa. Figure 6 shows that the width of the plastic zone of the coal pillar with both sides being mined out increased significantly with the increasing of the cover depth. For the geological conditions of longwall No. 52 303, when the cover depth reached 245 m (where the strong strata behaviour occurred, as is discussed in Section 3.4), the width of the plastic zone of the coal pillar increased to 17.5 m. In this condition, a coal pillar with a width of 20 m could hardly remain stable. A sufficiently wide elastic zone is needed to ensure the stability of the coal pillar.

3.2.2. Strength of and load on the coal pillar. The stability of the coal pillar is determined by the relation between the coal pillar strength and the load on the coal pillar. When the load on the coal pillar exceeds its strength, the coal pillar will be destroyed. According to Obert–Duvall formula (Obert & Duvall 1945a,b, 1967), the strength of the coal pillar, R, can be expressed as

$$R = R_c\left(0.778 + 0.222\frac{B}{h}\right) \quad (3)$$

where R_c is the cube compressive strength of the coal mass, and B and h are the width and height of the coal pillar, respectively.

Laboratory tests demonstrated that the cube compressive strength of the coal mass in the Daliuta coal mine was 19.5 MPa. The width and the height of the coal pillar were 20 and 7 m, respectively. Thus, the strength of the coal pillar in the Daliuta coal mine was 27.54 MPa, according to equation (3).

In the initial mining stage of longwall No. 52 303, the increment of the vertical stress induced by the extraction of longwall No. 52 303 was measured by underground workers, and provided a good reference point for this research. Two boreholes (Nos. 1 and 2) were drilled in the coal pillar between CRs No. 91 and No. 92, as detailed in figure 1. The drilling depths of the No. 1 and No. 2 boreholes were 2.7 and 9.5 m, respectively, with equal diameters of 42 mm. They were placed at 15-m intervals at a distance of 2.0 m from the floor. The initial values of the borehole stress meters were all set to zero. Unfortunately, due to equipment failure in No. 2 borehole, only the data from the No. 1 borehole was recorded successfully, as shown in figure 7. When the working face gradually approached the No. 1 monitoring point, beginning at 113 m behind the monitoring point and ending 20 m beyond it, the vertical stress dramatically increased from 0 to 7.3 MPa. This stress remained stable at around 7.0 MPa. However, the cover depth of the coal pillar between the No. 91 and No. 92 CRs was only 180 m (detailed in Section 3.4), and only increments of the vertical stress induced by the extraction of longwall No. 52 303 were measured, rather than the total amount of vertical stress. Therefore, FLAC^{3D} was utilized to reproduce the change in vertical stress within the coal pillar under the influence of the extraction of both longwalls No. 52 304 and No. 52 303 at different cover depths.

3.3. *Numerical simulation of the vertical stress in the coal pillar*

3.3.1. Establishment of the numerical models. Numerical models were established based on the geological setting of longwalls No. 52 303 and No. 52 304, and a few reasonable simplifications were made. The width, length, and height of the model were 300, 330,

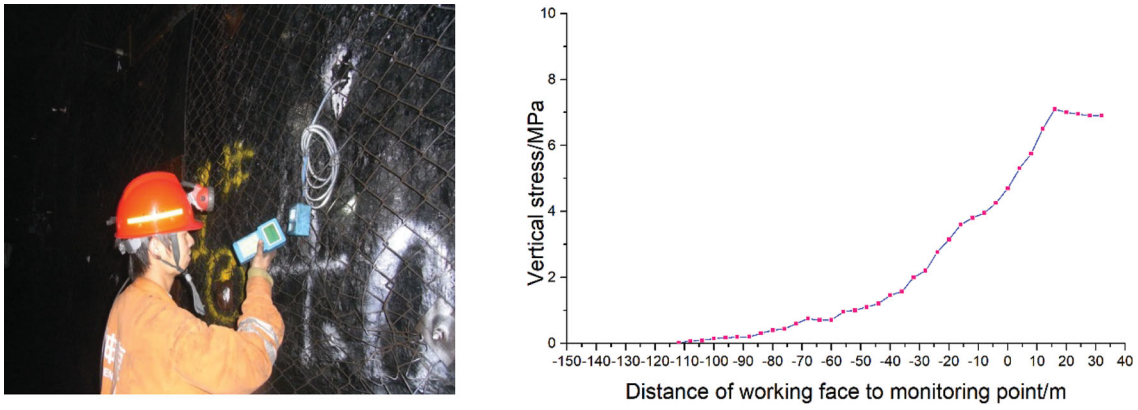

Figure 7. *In situ* monitoring and measured result of vertical stress: (a) *in situ* monitoring of vertical stress and (b) Measured result.

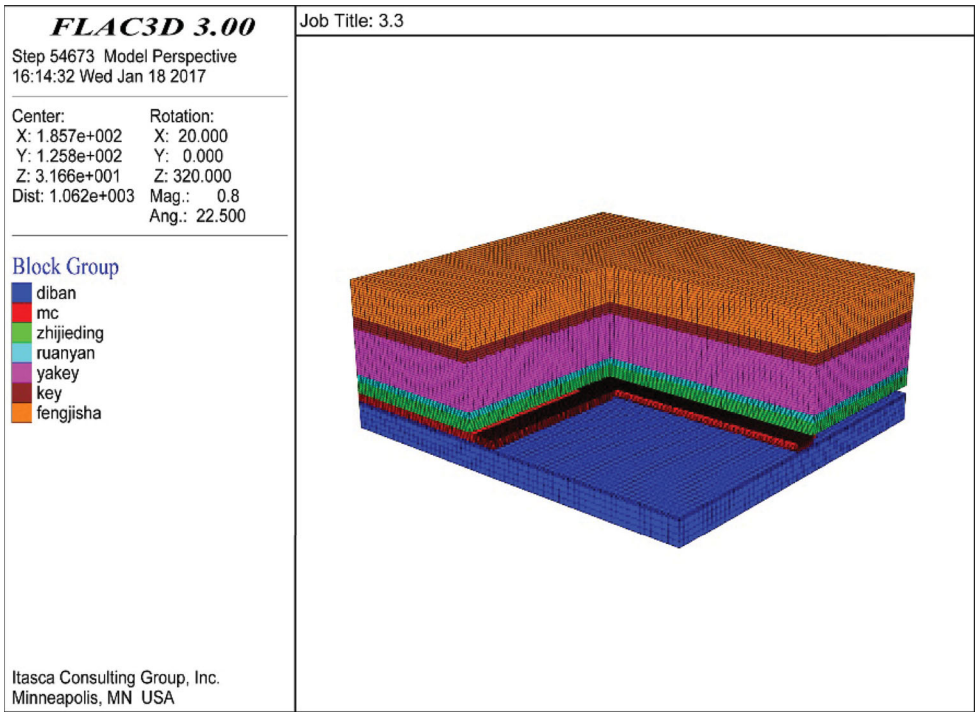

Figure 8. Layout of the numerical model.

and 124 m, respectively, as shown in figure 8. Each model contained two panels (i.e. the No. 52 303 and No. 52 304 longwall panels), and a row of 20-m wide, 50-m long coal pillars were built between them. All the roadways in the model were 5-m wide and 4-m high to be the same as in the real case. Uniformly distributed vertical stress with a gradient of 0.025 Mpa m^{-1} was applied to the top interface of the model to compensate for the load of the overlying strata. The dip angle of the strata was not considered because the coal seams in the Daliuta coal mine were relatively flat. The bottom boundary of the model was restricted in vertical movement, and the lateral boundary of the model was restricted in horizontal movement. All the remaining areas including the coal, the overlying strata and the floor were assumed to have elastic-perfectly plastic behaviour as defined by the Mohr–Coulomb strength criterion. Two models were established to simulate 180-m and 300-m cover depth scenarios to reproduce the change of vertical stress in the coal pillars at these two depths. The strata characteristics and mechanical parameters, including the thickness of stratum (T), elastic modulus (EM), Poisson's ratio (PR), internal friction angle (IFA), cohesion (C), tensile strength (TS) and unit weight (UW), are shown in Table 2.

3.3.2. Calculation and results of the numerical models. In the simulations, no coal pillars were left at the boundaries of the

Table 2. Mechanics parameter of each stratum in the numerical simulation.

Stratum lithology	T (m)	EM (GPa)	PR	IFA (deg)	C (MPa)	TS (MPa)	UW (t m^{-3})
Drift-sand	30	12	0.28	26	5.2	6	2.5
Key stratum 2	10	20	0.3	30	8	9	2.7
Weak stratum 2	38	15	0.26	23	7.5	5	2.3
Key stratum 1	6	20	0.3	30	8	9	2.7
Weak stratum 1	10	12	0.22	23	6	5	2.3
Coal seam	7	7.5	0.25	20	4.8	2	1.3
Floor	23	30	0.36	38	11	11	2.8

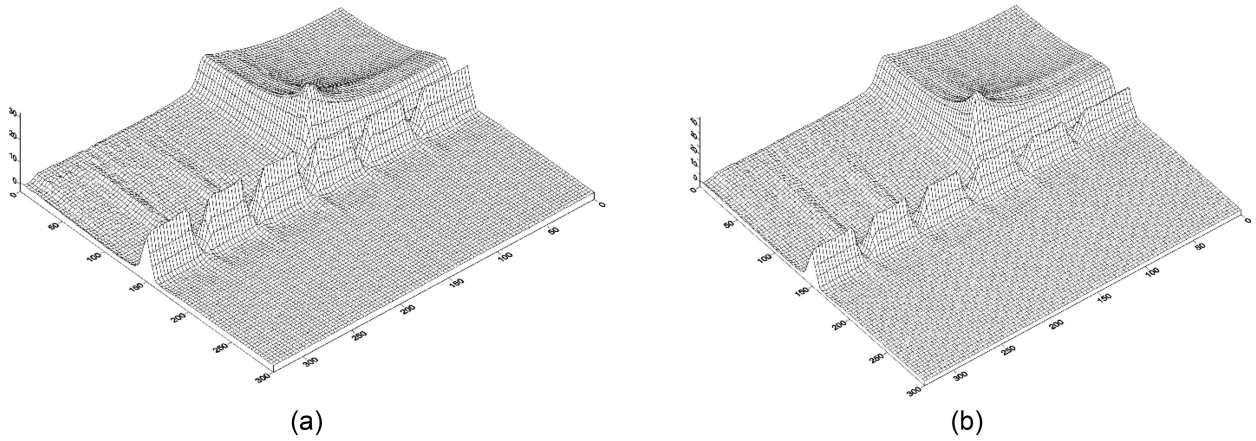

Figure 9. Vertical stress contour of the models: (a) Model No. 1 and (b) Model No. 2.

models during the extraction of the longwall panels. The No. 52 304 and No. 52 303 panels were successively excavated through 10-m steps in the simulation. The simulated excavation was stopped when the face of longwall No. 52 303 advanced to 175 m, and the last extraction step was 15 m. The stress monitoring point was set inside the coal pillar at an advancement distance of 155 m, and the position of the monitoring point was the same as that of the *in situ* monitoring so that the numerical simulation results could be validated through comparison with *in situ* data.

Figure 9 presents the vertical stress contours of two models, and the vertical stress data at each monitoring point are plotted in figure 10. Figure 10a shows that the trend of the vertical stress induced in the numerical simulation by the extraction of the No. 52 303 panel was the same as that in the *in situ* test with similar stress increments, indicating that the simulation results were reliable.

Figure 10 indicates that the vertical stress in the coal pillar increased significantly as the cover depth of the coal seam and the disturbance time increased. When the cover depth of the coal seam was 180 m (Model No. 1), the stress peaks of the monitoring points induced by the first and second mining were 14.56 and 17.04 MPa, respectively, neither of which exceeded the strength of the coal pillar, so the coal pillar remained stable. When the cover depth of the coal seam was 300 m (Model No. 2), the maximum of the vertical stress in the coal pillar did not exceed the strength of the coal pillar during the extraction of the first longwall panel. However, during the extraction of the second longwall panel, the vertical stress in the coal pillar quickly exceeded its strength ahead of the longwall face at 115 m. When the longwall face approached the monitoring point, the vertical stress in the coal pillar reached 42.4 MPa, which greatly exceeded the strength of the coal pillar. Therefore, the collapse of the coal pillar gave rise to the strong strata behaviour at the working face-end, as described in Section 3.1.

3.4. *Statistics of the conditions of the coal pillars in the Daliuta coal mine*

The theoretical analysis and numerical simulation results in the previous subsections show that the stability of the coal pillar was extremely sensitive to the cover depth, and depended on whether each side of the pillar had been mined out. Theoretical analysis suggests that it was the destruction of the coal pillar that triggered the strong strata behaviour that occurred at the face-end of longwall No. 52 303. However, the strong strata behaviour only occurred between the No. 21 and No. 12 CRs. To comprehensively determine the mechanism behind this incident, the detailed mining conditions of longwall No. 52 303 and similar longwall faces in the Daliuta coal mine were statistically analysed.

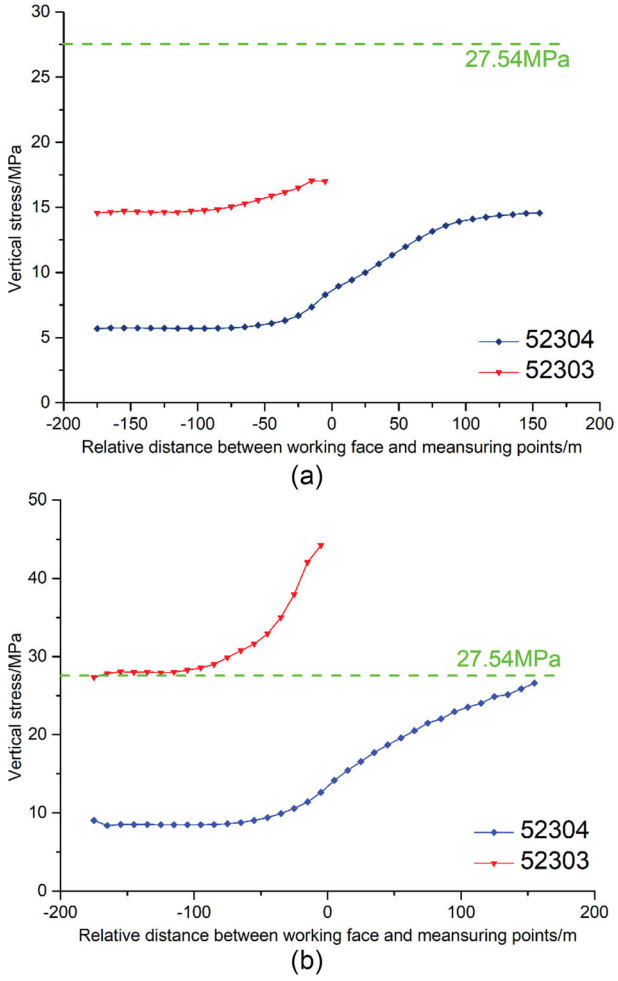

Figure 10. Plots of the vertical stress at each monitoring point: (a) Model No. 1 and (b) Model No. 2.

Figure 11 plots the change in cover depth of the coal pillar with the advancement of the working face. As shown in figure 11, after the No. 21 CR, the cover depths of the coal pillars began to exceed 245 m; and this value reached 280 m near the recovery roadway. Additionally, from the open-off cut to the No. 12 CR, all the coal pillars had been mined out on both sides, whereas the coal pillars between the No. 12 CR and the recovery roadway had only been mined out on one side. As described before, the strong strata behaviour occurred between the No. 21 and No. 12 CRs. Therefore, although the cover depths of the coal pillars between the No. 12 CR and the recovery roadway exceeded 265 m, the load borne by the coal pillars did not exceed their strength, so the coal pillars could remain stable. Because of this, the strong strata behaviour ceased after the No. 12 CR. Therefore, we conclude that the destruction of the coal pillars triggered the strong strata behaviour occurring at the longwall No. 52 303 working face-end.

To further demonstrate this conclusion, the maximum cover depths of the coal pillars with both sides mined out were measured from six longwall faces of the Daliuta coal mine, as presented in figure 12. The six working faces were mined in the following order: 52 304 → 52 303 → 52 305 → 52 302 → 52 306 → 52 307.

Figure 12 shows that the sequence of cover depths of the coal pillars from deep to shallow, with both sides being mined out in the six working faces, was 52 303 (264 m) → 52 302 (244.8 m) → 52 305 (243.3 m) → 52 306 (237.7 m) → 52 307 (235.5 m) → 52 304 (0 m). Among these six working faces, only the No. 52 303 working face had abnormally strong strata behaviour at the face-end. At that moment, the cover depth of the No. 52 303 working face was 245 m, and the cover depths of the coal pillars with both sides being mined out in other working faces were all less than 245 m, indicating that a cover depth of 245 m might be a threshold for this type of strong strata behaviour. Therefore, for the geological settings and mining conditions of the Daliuta coal mine, where the mining heights of the working face and the width of the coal pillars are normally 7.0 and 20 m, respectively, the critical cover depth value to prevent strong strata behaviour is 245 m.

4. Countermeasures for controlling strong strata behaviour

In the Daliuta coal mine, there still exist numerous 7.0-m-high longwall panels that need to be mined. Therefore, to prevent the occurrence of strong strata behaviour and advance roadway deformation, it is necessary to identify countermeasures that can control the strong strata behaviour at the working face-ends.

According to the above results, the destruction of the coal pillars behind the working face causes the face-end strong strata behaviour and the advance roadway deformation. Therefore, in the design of future longwall panels, the distribution of the cover depth of the coal seam in each panel should be investigated in detail. In regions where the cover depths exceed 245 m, the existing design of coal pillars with a width of 20 m would no longer be safe. Countermeasures proposed below could be used to prevent incidents that might occur when mining longwalls with similar conditions.

Increasing the width of the coal pillar is the easiest method to prevent this kind of strong strata behaviour, although this would also reduce the recovery rate of the coal resources. According to the geological settings of the No. 5-2 coal seam in the Daliuta coal mine, the maximum cover depth of the coal pillars with both sides being mined out is 265 m. According to equation (2), the width of the plastic zone of the coal pillar with both sides being mined out is 21 m. Current engineering standards (Qian *et al.* 2010) suggest that an elastic zone with height twice that of the roadway can guarantee the stability of the coal pillar. Therefore, for the No. 5-2 coal seam in the Daliuta coal mine, the width of the coal pillar should

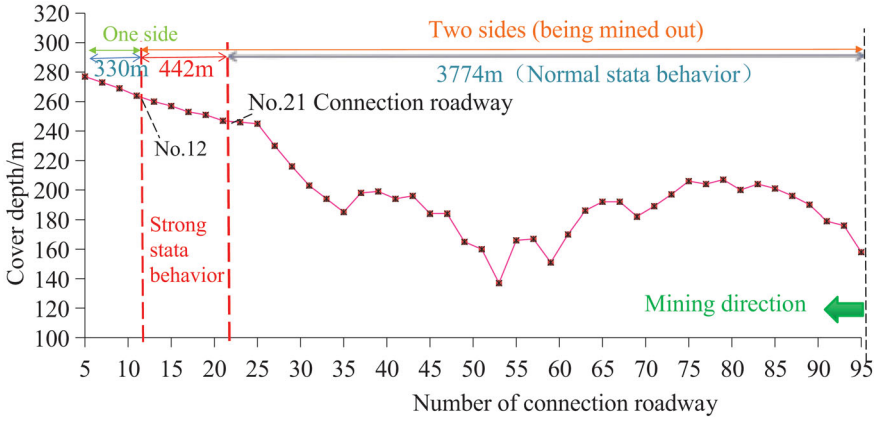

Figure 11. The relation between cover depth of coal pillars, strong strata behaviour and the condition of sides mined in longwall No. 52 303.

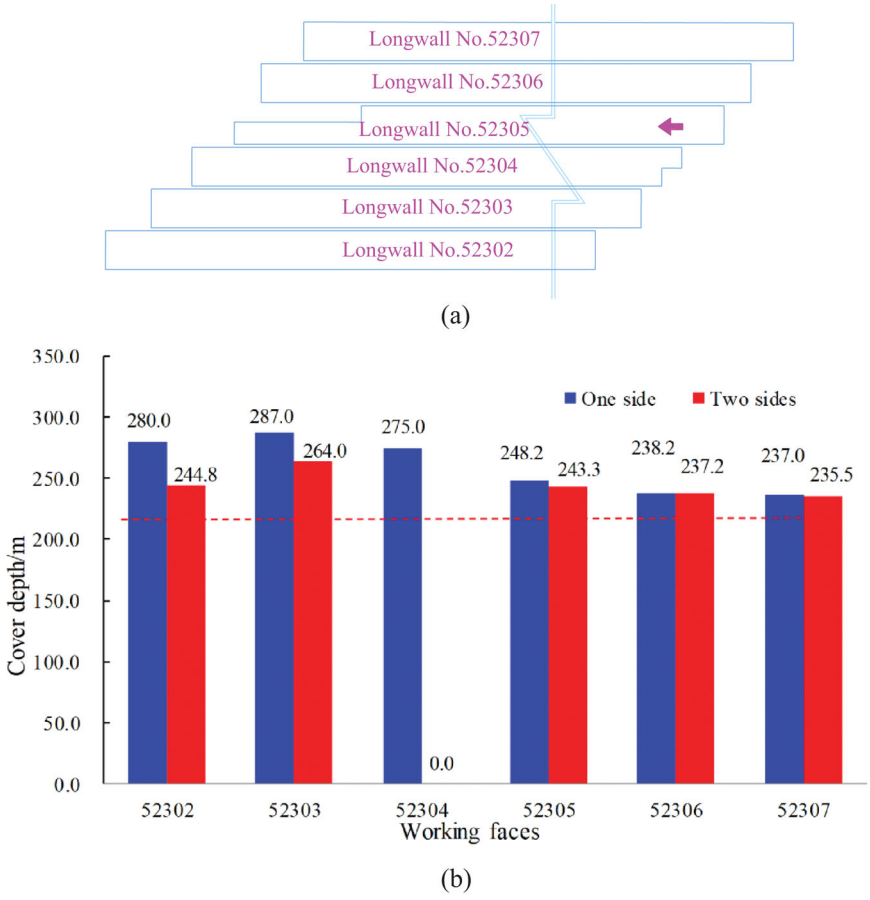

Figure 12. Relative position and maximum cover depths of six working faces in the Daliuta coal mine: (a) relative position and (b) maximum cover depths.

be at least 29 m. Aside from increasing the width of the coal pillar, advance grout injection into the pillar is another way to increase the strength of the coal pillars. The boreholes for injecting grout can be drilled in advance, ahead of the working face 1–2 CRs.

From the perspective of reducing the load on the coal pillars, implementing advance destress blasting to the main roof above the current longwall face and the adjacent goaf is also an effective way to prevent the destruction of the coal pillars, as shown in figure 13. After blasting, the broken blocks of the overlying key strata cannot overlap above the coal pillars, thereby reducing the load on them.

Apart from the countermeasures mentioned above, other auxiliary measures, such as increasing the densities of

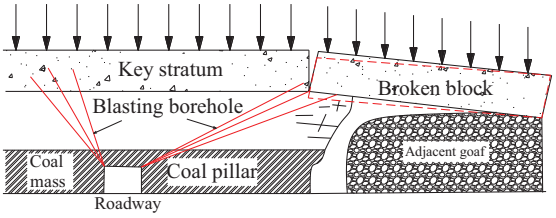

Figure 13. Advance destress blasting to the main roof.

anchors and cables, and adding W-shaped steel belts in the supporting of the roadway, can also be taken during the extraction of the No. 5-2 coal seam in the Daliuta coal mine. Others have discussed these measures in detail (He *et al.* 2005; Jiang *et al.* 2005), and thus they are not presented here.

5. Conclusions

The Shendong mining area is a typical mining area with shallow coal seams. The Daliuta coal mine, one of the biggest coal mines in this area, generally uses a fully mechanized mining method with a high mining height (7.0 m) to extract coal resources, greatly improving production efficiency. However, when the mining depth is gradually increased, the end regions of some longwalls, such as longwall No. 52 303, suffered abnormally strong strata behaviours. These behaviours included roof collapse and advance roadway deformation, even triggering breakages and failures of the individual advance props, which significantly delayed the safe and efficient production of the mine.

By analysing the breakage structures and movement characteristics of the overlying strata above the working face-ends, we observed that instability of the coal pillar was the root cause of the abnormally strong strata behaviour presented in this paper. Theoretical analysis and numerical simulation demonstrated that the stability of the coal pillar with a certain width was extremely sensitive to the cover depth, and that the stability also depended on whether both sides of the pillar had been mined out. For shallow coal seams in the Shendong mining area, there exists a threshold for the cover depth when both sides of a coal pillar are mined out. When the mining depth exceeds this threshold, the coal pillars become unstable, which results in the strong strata behaviour at the working face-ends.

Field measurements and statistical analyses suggest a cover depth threshold of 245 m for 20-m wide coal pillars if both sides of the coal pillar are mined out. In regions where the cover depths of the coal seams exceed 245 m, targeted countermeasures can be used to prevent the strong strata behaviour. These methods include increasing the width of the coal pillar, advance grout injection into the coal pillar and advance destress blasting to the main roof above the current working face and the adjacent goaf. The proposed solutions may facilitate future safe mining of shallow coal seams widely distributed across the world.

Acknowledgements

Financial supports from the Fundamental Research Funds for the Central Universities (2017XKQY023) are greatly appreciated.

Conflict of interest statement. None declared.

References

Bai, J., 2006. *Surrounding Rock Control of Entry Driven Along Goaf*, China University of Mining and Technology Press, Xuzhou, pp. 19–20.

Bieniawski, Z., 1986. *Strata Control in Mineral Engineering*, John Wiley and Sons Inc., New York.

Gao, W., 2014. Study on the width of the non-elastic zone in inclined coal pillar for strip mining, *International Journal of Rock Mechanics and Mining Sciences*, **72**, 304–310.

Han, C., Zhang, N., Ran, Z., Gao, R. & Yang, H., 2018. Superposed disturbance mechanism of sequential overlying strata collapse for gob-side entry retaining and corresponding control strategies, *Journal of Central South University*, **25**, 2258–2271.

He, M., Xie, H., Peng, S. & Jiang, Y., 2005. Study on rock mechanics in deep mining engineering, *Chinese Journal of Rock Mechanics and Engineering*, **24**, 2803–2813.

Hou, Z., 2000. Analysis of combinatorial key strata stability in shallow coal seam with thick loose bed, *Journal of China Coal Society*, **25**, 127–131.

Huang, Q., 2002. Ground pressure behavior and definition of shallow seams, *Chinese Journal of Rock Mechanics and Engineering*, **21**, 1174–1177.

Jia, S., Wang, J. & Zhu, J., 2011. Calculation and application on elastic-plastic coal pillar width of the stope, *Procedia Engineering*, **26**, 1116–1124.

Jiang, Y., Liu, W., Zhao, Y., Yin, Z., Li, J., Deng, Z. & Hong, Y., 2005. Study on surrounding rock stability of deep mining in Kailuan group, *Chinese Journal of Rock Mechanics and Engineering*, **24**, 1857–1862.

Ju, J., Xu, J. & Shan, Z., 2015a. Mechanisms of the abnormal first weighting in 'knife handle shaped face' with 7.0 m high supports, *International Journal of Oil, Gas and Coal Technology*, **9**, 348–358.

Ju, J., Xu, J. & Zhu, W., 2015b. Longwall chock sudden closure incident below coal pillar of adjacent upper mined coal seam under shallow cover in the Shendong coalfield, *International Journal of Rock Mechanics and Mining Sciences*, **77**, 192–201.

Li, Z., Xu, J., Yu, S., Ju, J. & Xu, J., 2018. Mechanism and prevention of a chock support failure in the longwall top-coal caving faces: a case study in Datong coalfield, *China Energies*, **11**, 288.

Malan, F., 1998. Ultra-deep mining: the increased potential for squeezing conditions, *Journal of The South African Institute of Mining and Metallurgy*, **98**, 353–363.

Masoud, S., Parviz, M. & Ebrahim, Y., 2016. Optimizing and slope determination of final wall for Maiduk Mine with consideration of destabilizer factors, *International Journal of Mining Science and Technology*, **26**, 501–509.

Meng, Z., Shi, X. & Li, G., 2016. Deformation, failure and permeability of coal-bearing strata during longwall mining, *Engineering Geology*, **208**, 69–80.

Mudd, G., 2010. The environmental sustainability of mining in Australia: key mega-trends and looming constraints, *Resources Policy*, **35**, 98–115.

Obert, L. & Duvall, W., 1945a. *The Microseismic method of predicting rock failures in underground mining, Part 1, General Method*, U.S. Bureau of Mines, RI 3797.

Obert, L. & Duvall, W., 1945b. *The Microseismic method of predicting rock failures in underground mining, Part 2, Laboratory Experiments*, U.S. Bureau of Mines, RI 3803.

Obert, L. & Duvall, W., 1967. *Rock Mechanics and the Design of Structures in Rock*, John Wiley and Sons, Inc., New York, pp. 113–188.

Peng, S., 1978. *Coal Mine Ground Control*, John Wiley and Sons Inc., New York.

Qian, M., Shi, P. & Xu, J., 2010. *Ground Pressure and Strata Control*, China University of Mining and Technology Press, Xuzhou.

Qu, Q., Xu, J., Wu, R., Qin, W. & Hu, G., 2015. Three-zone characterisation of coupled strata and gas behaviour in multi-seam mining, *International Journal of Rock Mechanics and Mining Sciences*, **78**, 91–98.

Singh, R., Mandal, P., Singh, A., Kumar, R., Maiti, J. & Ghosh, A., 2008. Upshot of strata movement during underground mining of a thick coal seam below hilly terrain, *International Journal of Rock Mechanics and Mining Sciences*, **45**, 29–46.

Xie, J., Xu, J. & Wang, F., 2018. Mining-induced stress distribution of the working face in a kilometer-deep coal mine–a case study in Tangshan coal mine, *Journal of Geophysics and Engineering*, **15**, 2060–2070.

Xu, C., Yuan, L., Cheng, Y., Wang, K., Zhou, A. & Shu, L., 2016. Square-form structure failure model of mining-affected hard rock strata: theoretical derivation, application and verification, *Environmental and Earth Science*, **75**, 1180.

Xu, J., Zhu, W. & Ju, J., 2017. Mechanism of dynamic mine pressure occurring below adjacent upper chamber mining goaf with shallow cover depth, *Journal of China Coal Society*, **42**, 500–509.

Xu, J., Zhu, W. & Ju, J., 2014. Supports crushing types in the longwall mining of shallow seams, *Journal of China Coal Society*, **39**, 1625–1634.

Xu, J., Zhu, W., Wang, X. & Zhang, Z., 2012. Influencing mechanism of gully terrain on ground pressure behaviors in shallow seam longwall mining, *Journal of China Coal Society*, **37**, 79–85.

Xuan, D., Xu, J., Wang, B. & Teng, H., 2015. Borehole investigation of the effectiveness of grout injection technology on coal mine subsidence control, *Rock Mechanics and Rock Engineering*, **48**, 2435–2445.

Xuan, D. & Xu, J., 2017. Longwall surface subsidence control by technology of isolated overburden grout injection, *International Journal of Mining Science and Technology*, **27**, 813–818.

Yang, J., Liu, C., Yu, B. & Wu, F., 2016. An analysis on strong strata behaviors and stress transfer of the roadway approaching gob in triangle area of the face end, *Journal of Mining and Safety Engineering*, **33**, 88–95.

Yang, P. & Liu, C., 2012. Structure forms of basic roof and reasonable supporting parameters in ends of fully-mechanized top caving face, *Journal of Mining and Safety Engineering*, **29**, 26–32.

Yu, B., Zhu, W., Gao, R. & Liu, J., 2016. Strata structure and its effect mechanism of large space stope for fully mechanized sublevel caving mining of extremely thick coal seam, *Journal of China Coal Society*, **41**, 571–580.

Zhu, W., 2011. Study on the instability mechanism of key strata structure in repeating mining of shallow close distance seams, *Journal of China Coal Society*, **36**, 1065–1066.

Zhu, W., Chen, L., Zhou, Z., Shen, B. & Xu, Y., 2018a. Failure propagation of pillars and roof in a room and pillar mine induced by longwall mining in the lower seam, *Rock Mechanics and Rock Engineering*, **52**, 1193–1209.

Zhu, W., Ren, D. & Chen, M., 2015. Rational buried depth for regulating roadway application during coal face withdrawal in Shendong mining area, *Journal of Mining and Safety Engineering*, **32**, 279–284.

Zhu, W., Xu, J. & Xu, G., 2017a. Mechanism and control of roof fall and support failure incidents occurring near longwall recovery roadways, *Journal of The South African Institute of Mining and Metallurgy*, **117**, 1063–1072.

Zhu, W., Xu, J. & Li, Y., 2017b. Mechanism of the dynamic pressure caused by the instability of upper chamber coal pillars in Shendong coalfield, China, *Geosciences Journal*, **21**, 729–741.

Zhu, W., Xu, J., Xu, J., Chen, D. & Shi, J., 2017c. Pier-column backfill mining technology for controlling surface subsidence, *International Journal of Rock Mechanics and Mining Sciences*, **96**, 58–65.

Zhu, W., Yu, S. & Xu, J., 2018b. Influence of the elastic dilatation of mining-induced unloading rock mass on the development of bed separation. *Energies*, **11**, 785.

Zhu, W., Xu, J., Ju, J. & Qu, Q., 2018c. *Strong Weighting Events in Shallow Multi-seam Longwall Mining*, 18th Coal Operators' Conference, University of Wollongong Australia, pp. 112–118.